

Reconstruction of the Scale and Chronology of the Woda Paleo-Landslide-Dammed Lake in the Upper Jinsha River

Li Qin Zhou^{1,2}, Mingyue Qin^{3*}

¹Key Laboratory of Mountain Hazards and Surface Process, Institute of Mountain Hazards and Environment, Chinese Academy of Sciences, Chengdu, 610041, China

²University of Chinese Academy of Sciences, Beijing, 100149, China

³Sichuan Chuangao Engineering Technology Consulting CO.,LTD., Chengdu, 610095, China

*Corresponding author: qinmingyuecg@163.com

Abstract: The upper Jinsha River in the southeastern margin of the Tibetan Plateau, characterized by intense tectonic activity and steep terrain, is a high-risk zone for landslide-damming events. This study focuses on the Woda paleo-landslide-dammed lake, reconstructing its chronology, scale, and geomorphic effects through optically stimulated luminescence (OSL) dating and a "dam-lake synergy analysis." OSL dating results indicate that the landslide-damming event occurred at ~60 ka, corresponding to the late Marine Isotope Stage 4 (MIS 4). During this period, diurnal temperature fluctuations near freezing thresholds promoted repeated freeze-thaw cycles, accelerating bedrock fracturing and preconditioning slope instability. The landslide involved a volume of $1.93 \times 10^8 \text{ m}^3$, forming a 109-m-high dam that impounded a lake with a maximum surface area of $21.04 \times 10^6 \text{ m}^2$ and storage capacity of $137.61 \times 10^7 \text{ m}^3$. Lacustrine sediments indicate a minimum water level corresponding to a reduced area of $11.93 \times 10^6 \text{ m}^2$ and capacity of $53.03 \times 10^7 \text{ m}^3$. A 42-m vertical difference between the frontal dam elevation (3,100 m a.s.l.) and the top of lacustrine deposits (3,058 m a.s.l.), combined with evidence of rapid sediment accumulation, suggests short-lived lake existence followed by catastrophic dam breaching. By integrating landslide dam morphology, lacustrine stratigraphy, and multi-proxy sedimentary evidence, this study addresses systematic biases inherent to traditional lacustrine sediment-based reconstructions. It reveals the triggering mechanism of mega-landslides driven by climate-tectonic coupling and provides a methodological framework for assessing landslide-flood cascading hazards in tectonically active regions. The findings underscore the need to address slope destabilization risks induced by freeze-thaw processes under current climate warming.

Keywords: Paleo Landslide Dam, Paleo Dammed Lake Reconstruction, OSL Dating, Upper Jinsha River

1. Introduction

Landslide-damming events, as low-frequency, high-impact geological disasters, often trigger outburst floods that damage ecological environments and infrastructure, threatening human lives and property safety. On October 11 and November 3, 2018, two large-scale high-position landslides successively occurred on the right bank of the Jinsha River at the border between Jiangda County, Tibet Autonomous Region, and Baiyu County, Sichuan Province, forming the Baige landslide-dammed lake, one of China's most representative river-blocking events in recent years [1]. The resulting outburst floods severely damaged downstream riverside roads, bridges, and farmland, causing significant economic losses. Paleo-landslide-dammed lakes are widespread in mountainous regions [2]. Current research on paleo-landslide-dammed lakes primarily focuses on the eastern Tibetan Plateau, particularly within large river valleys such as the upper reaches of the Yellow River, Min River, Jinsha River, and Dadou River [3-9]. Although dating tests have been conducted for most paleo-dammed lakes, studies on their scale and long-term geomorphic effects remain relatively limited.

The upper Jinsha River, located in the Hengduan Mountains on the eastern margin of the Tibetan Plateau, is one of the most tectonically active and topographically steep regions globally, favoring the occurrence of landslide-damming events [10]. Residual landslide dam deposits and lacustrine sediments serve as key evidence for identifying paleo landslide damming events [8, 11]. Fine-grained lacustrine deposits (silt-clay layers) along the riverbanks, combined with their elevation above the river and topographic data, can reconstruct paleo dammed lake levels, surface area, and storage capacity [7, 9].

However, lacustrine sediments often only record residual or post-breach minimum water levels [12], potentially leading to underestimation of the original lake dimensions [13]. Recent studies integrating lacustrine, fan-delta, and outburst flood sedimentary profiles, along with dam breach morphology, have reconstructed the scale and chronology of paleo-landslide-dammed lakes in the Parlung Tsangpo River basin, improving reconstruction accuracy [12, 14]. Therefore, this study employs field investigations and optically stimulated luminescence (OSL) dating to reconstruct the age and dimensions of the Woda paleo-landslide along the upper Jinsha River. This study has pioneered a reconstruction framework for paleo landslide damming events, aiming to restore extreme river-blocking phenomena absent in modern observational records, thereby extending the frequency-magnitude distribution spectrum of geomorphic hazards in the southeastern Tibetan Plateau.

2. Regional setting

The upper Jinsha River segment spans approximately 381 km from the Batang River confluence in Yushu, Qinghai Province to Baiyu County, Sichuan Province, traversing Qinghai, Tibet, and Sichuan provinces (Figure 1). Situated in the eastern margin of the Tibetan Plateau within the "Three Parallel Rivers" World Heritage core zone, it forms a tectonic-ecological transitional belt between the plateau interior and Yunnan-Guizhou Plateau. This region, flanked by the Lancang River to the west and Yalong River to the east, exemplifies the characteristic "alternating mountains and valleys" morphology of the Hengduan Mountains.

Structurally controlled by the active Jinsha River Fault Zone and Ganzi-Yushu Fault Zone, the area exhibits neotectonic uplift rates of 3-5 mm/a, dominated by sinistral strike-slip motion with thrust components. Historic seismic events, including the 2010 Yushu earthquake (Mw 6.9) and 1896 Shiqu earthquake (Mw 7.3), have generated widespread slope instabilities. The intense tectonic compression has sculpted a >2,000 m relief landscape featuring deeply incised V-shaped valleys with steep slopes (30°-60°), entrenched meanders, and discontinuous fluvial terraces-geomorphic signatures reflecting the interplay between episodic tectonic uplift and rapid fluvial incision since the Late Pleistocene [15].

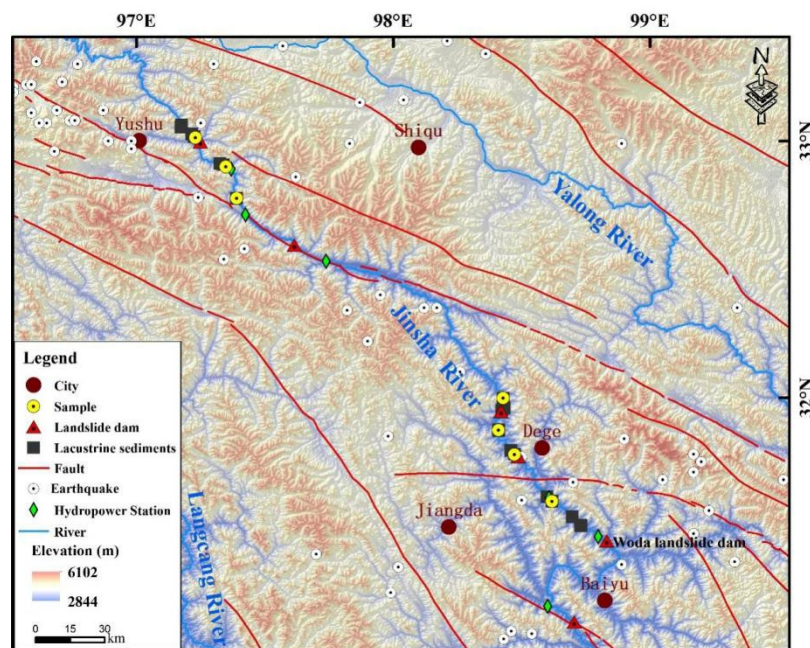


Figure 1 Study Area Overview Map

3. Method

3.1 Optically-stimulated luminescence dating

Three OSL samples from sections were analyzed to constrain the chronology of dammed-lake events. Following Lai and Ou (2013) [16], quartz grains (38-63 μm) were chemically purified under red light and measured using a Lexsyg Research Reader. The SAR protocol [17] and SGC method [18-19] were

applied to determine equivalent doses (De), with preheating at 220°C (test dose) and 260°C (natural/regenerative doses). Dose rates incorporated U/Th/K concentrations (neutron activation analysis), $15 \pm 5\%$ water content [20], cosmic ray contributions [21], and an α -value of 0.035 [22].

3.2 Reconstruction of paleo landslide dammed lake scale

Conventional methods for reconstructing paleo-lake levels, which rely predominantly on the elevation of lacustrine sediments, exhibit significant limitations. Statistical studies indicate that approximately 27% of landslide dams breach within 1 day and 50% fail within 10 days of formation [23], resulting in lacustrine deposits that often only record residual or post-breach minimum water levels [12]. This systematic bias leads to substantial underestimation of the original lake dimensions [13]. To mitigate these constraints, this study adopts a "dam-lake synergy analysis" approach, integrating geomorphic constraints from both the landslide dam morphology and lacustrine sedimentary records. The maximum potential water level is defined by the frontal elevation of the landslide dam, while the minimum stable water level is calibrated using the top elevation of intact lacustrine sediments. Lake surface area was delineated by mapping elevation contours (30-m resolution SRTM DEM data) in ArcGIS 10.2, followed by DEM clipping to extract the inundation extent. Storage capacity was subsequently calculated using the Surface Volume tool within the 3D Analyst module, which quantifies volumetric relationships between elevation, surface area, and depth across the impounded basin.

4. Result

4.1 Characteristics of the Landslide Dam

Discovered near Baiyu County, the Woda landslide dam ($31^{\circ}26'30.74''$, $98^{\circ}49'52.30''$) on the Jinsha River's right bank exhibits a 662-m vertical drop from its source (3,653 m) to toe (2,991 m), with asymmetric remnants (right bank: 3,590 m; left bank: 3,100 m) and a 109-m dam height (Figure 2). The deposit ($2.14 \times 10^6 \text{ m}^2$, $1.93 \times 10^8 \text{ m}^3$) comprises phyllite, sandstone, siliceous rocks, limestone, and intermediate-mafic volcanics, suggesting failure preconditioned by weak metasedimentary layers and tectonic fracturing. Classified as a colossal rockslide (Cruden-Varnes Type V), its geometry implies high-energy emplacement linked to Jinsha River valley incision dynamics.



Figure 2 Aerial photograph of the Woda landslide

4.2 Geochronological results of the dammed lake

An extensive succession of continuous lacustrine deposits was identified upstream of the Woda landslide complex. For chronological analysis, three optically stimulated luminescence (OSL) samples were systematically collected from a representative lacustrine sedimentary profile (Figure 3), with corresponding dating results summarized in Table 1. The 8.5-m-thick stratigraphic column exhibits a well-defined vertical succession. Unit 1 (0-2.3 m): Colluvial deposits dominated by matrix-supported

angular debris; Unit 2 (2.3-4.7 m): Heterogeneous diamicton comprising angular lithic clasts (20-50 cm diameter) interstratified with subrounded fluvial gravels, displaying weak imbrication; Unit 3 (4.7-5.9 m): A distinct 1.2-m-thick clay-dominated lacustrine sequence characterized by millimeter-scale laminations and pervasive iron-manganese staining; Unit 4 (5.9-8.5 m): Basal fluvial conglomerate layer exhibiting well-developed imbricated structures and clast-supported fabric.

Table 1 Optically stimulated luminescence (OSL) dating results

Sample ID	Depth (m)	Water content (%)	particle size	K (%)	Th (ppm)	U (ppm)	Dose rate(Gy/ka)	De (Gy)	Age (ka)
JS23-20	5.80	15±5	38-63	1.58±0.08	7.41±0.37	2.08±0.10	2.47±0.18	150.55±5.55	61.01±5.09
JS23-21	7.10	15±5	38-63	1.63±0.08	7.88±0.39	2.14±0.11	2.53±0.19	151.91±9.32	59.99±5.83
JS23-22	7.60	15±5	38-63	1.49±0.07	7.29±0.36	2.04±0.10	2.35±0.18	142.50±3.89	60.61±4.85

Three OSL samples (JS23-20, JS23-21, JS23-22) collected vertically through the lacustrine unit (Unit 3) yielded statistically consistent ages of 61.01 ka, 59.99 ka and 60.61 ka respectively. This chronological coherence (all ages overlapping at 1 σ uncertainty) strongly supports a singular geomorphic event at ~60 ka when the Woda landslide episodically blocked the Jinsha River-a major tectonically controlled valley. The lacustrine depositional package (Unit 3) likely represents suspended load accumulation within a short-lived landslide-dammed lake, while the overlying diamicton (Unit 2) reflects subsequent fluvial reworking phase following dam breaching. The remarkable age clustering further implies rapid sediment accumulation (<2 ka) post-damming, consistent with catastrophic landslide emplacement dynamics in active orogenic settings.



Figure 3 Sampling section of Woda Landslide dammed Lake

5. Discussion

Based on field investigations, The maximum and minimum inundation extents of the Woda landslide-dammed lake were reconstructed by integrating the elevation of the lacustrine deposit tops and the landslide dam morphology (Figure 4). The highest elevation of lacustrine sediments upstream of the Woda landslide dam was identified at 3,058 m above sea level (a.s.l.). This elevation was adopted as the minimum paleo-lake level to reconstruct the dammed lake's basal dimensions, yielding a minimum lake surface area of $11.93 \times 10^6 \text{ m}^2$ and a storage capacity of $53.03 \times 10^7 \text{ m}^3$. Conversely, the elevation of the woda landslide dam (3,100 m a.s.l.) was used to infer the maximum potential lake level, corresponding to an expanded surface area of $21.04 \times 10^6 \text{ m}^2$ and a maximum storage capacity of $137.61 \times 10^7 \text{ m}^3$. Using classical formula-based estimation [6], the peak discharge of the dam-break flood was calculated to range

from $3.13 \times 10^4 \text{ m}^3/\text{s}$ (minimum) to $6.12 \times 10^4 \text{ m}^3/\text{s}$ (maximum). The 42-m vertical difference between these two reconstructed lake levels highlights a dramatic reduction in reservoir volume, strongly suggesting catastrophic dam breaching shortly after the lake formation.

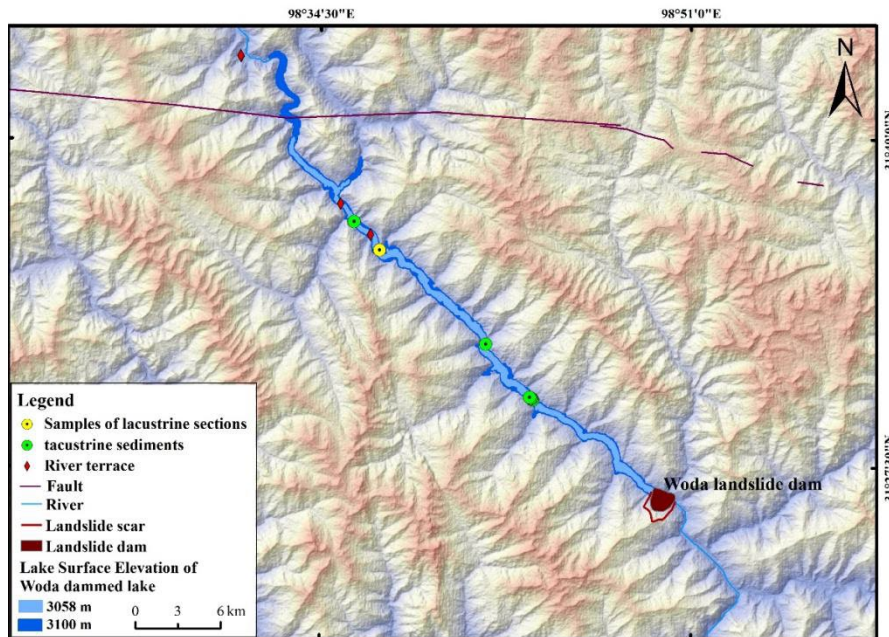


Figure 4 Paleo-extent of the Woda dammed lake

The geochronological coherence of OSL ages ($\sim 60 \text{ ka}$) from the lacustrine unit indicates that the Woda landslide-dammed lake existed for a geologically brief period, consistent with ephemeral dammed lakes in high-relief fluvial systems. This timing coincides with the late Marine Isotope Stage 4 (MIS 4: 71-57 ka), a transitional phase characterized by fluctuating daily temperatures near freezing thresholds. Such thermal regimes would have promoted frost weathering through repeated diurnal freeze-thaw cycles, accelerating bedrock fracturing and preconditioning slope instability. Enhanced cryogenic processes likely facilitated the development of detachment surfaces within fractured bedrock, ultimately triggering the Woda landslide. This study underscores the interplay between Late Pleistocene climatic oscillations and slope destabilization in the southeastern Tibetan Plateau, providing a mechanistic framework for evaluating recurrence intervals of similar paleo-hazards in climate-sensitive mountainous regions.

6. Conclusion

This study reconstructs the $\sim 60 \text{ ka}$ Woda landslide-damming event in the upper Jinsha River using OSL dating and a "dam-lake synergy" approach, revealing its geomorphic and climatic drivers. Coherent OSL ages correspond to the late MIS 4, during which diurnal freeze-thaw cycles under near-freezing temperatures enhanced bedrock fracturing, preconditioning slope failure. The landslide mobilized $1.93 \times 10^8 \text{ m}^3$ of rock, forming a 109-m-high dam that impounded a lake with a maximum area of $21.04 \times 10^6 \text{ m}^2$ and storage capacity of $137.61 \times 10^7 \text{ m}^3$. A 42-m elevation difference between the dam crest (3,100 m) and lacustrine sediments (3,058 m) indicates rapid breaching, releasing catastrophic floods comparable to historic megafloods. By integrating dam morphology, lacustrine stratigraphy, and chronometric data, this study overcomes limitations of single-proxy methods, refining paleo-hazard estimates of frequency and magnitude. The event highlights coupled climate-tectonic controls: tectonic uplift along the Jinsha River Fault Zone created steep topography, while MIS 4 thermal fluctuations triggered slope instability. These findings underscore the persistent risk of cascading hazards (landslide-damming-outburst floods) in active orogens under climatic shifts.

References

- [1] Ouyang C, An H, Zhou S, et al. Insights from the failure and dynamic characteristics of two sequential landslides at Baige village along the Jinsha River, China[J]. *Landslides*, 2019, 16: 1397-1414.
- [2] Korup O and Tweed F. Ice, moraine, and landslide dams in mountainous terrain[J]. *Quaternary*

Science Reviews, 2007, 26(25-28): 3406-3422.

[3] Guo X, Sun Z, Lai Z, et al. Optical dating of landslide-dammed lake deposits in the upper Yellow River, Qinghai-Tibetan Plateau, China[J]. *Quaternary International*, 2016, 392: 233-238.

[4] Jiang H, Xue M, Xu H, et al. Provenance and earthquake signature of the last deglacial Xinmocun lacustrine sediments at Diexi, East Tibet[J]. *Geomorphology*, 2014, 204(1): 518-531.

[5] Ping W, Zhang B, Qiu W, et al. Soft-sediment deformation structures from the Diexi paleo-dammed lakes in the upper reaches of the Minjiang River, east Tibet[J]. *Journal of Asian Earth Sciences*, 2011, 40(4): 865-872.

[6] Liu W, Carling P A, Hu K, et al. Outburst floods in China: A review[J]. *Earth-Science Reviews*, 2019, 197: 102895.

[7] Liu W, Hu K, Carling P A, et al. The establishment and influence of Baimakou paleo-dam in an upstream reach of the Yangtze River, southeastern margin of the Tibetan Plateau[J]. *Geomorphology*, 2018, 321(15): 167-173.

[8] Li Y, Chen J, Zhou F, et al. Identification of ancient river-blocking events and analysis of the mechanisms for the formation of landslide dams in the Suwalong section of the upper Jinsha River, SE Tibetan Plateau[J]. *Geomorphology*, 2020, 368: 107351.

[9] Wang H, Tong K, Hu G, et al. Dam and megafloods at the First Bend of the Yangtze River since the Last Glacial Maximum[J]. *Geomorphology*, 2020, 373(15): 107491.

[10] Xia M, Ren G M and Tian F. Mechanism of an ancient river-damming landslide at batang hydropower station, Jinsha river basin, China[J]. *Landslides*, 2023, 20(10): 2213-2226.

[11] Scherler D, Munack H, Mey J, et al. Ice dams, outburst floods, and glacial incision at the western margin of the Tibetan Plateau: A > 100 k.y. chronology from the Shyok Valley, Karakoram[J]. *Geological Society of America Bulletin*, 2014, 126(5-6): 738-758.

[12] Wang H, Cui P, Liu D, et al. Evolution of a landslide-dammed lake on the southeastern Tibetan Plateau and its influence on river longitudinal profiles[J]. *Geomorphology*, 2019, 343: 15-32.

[13] Johnsen T F and Brennand T A. The environment in and around ice-dammed lakes in the moderately high relief setting of the southern Canadian Cordillera[J]. *Boreas*, 2006, 35(1): 106-125.

[14] Wang H, Cui P, Zhou L, et al. Spatial and temporal distribution of landslide-dammed lakes in Purlung Tsangpo[J]. *Engineering Geology*, 2022, 308: 106802.

[15] Yu Y, Wang X, Yi S, et al. Late Quaternary aggradation and incision in the headwaters of the Yangtze River, eastern Tibetan Plateau, China[J]. *Bulletin*, 2022, 134(1-2): 371-388.

[16] Lai, Z. and Ou, X. Basic procedures of optically stimulated luminescence (OSL) dating. *Progress in Geography*, 2013, 32: 683-693.

[17] Murray, A.S. and Wintle, A. Luminescence dating of quartz using an improved single-aliquot regenerative-dose protocol. *Radiation Measurements*, 2000, 32(1): 57-73.

[18] Lai, Z., 2006. Testing the use of an OSL standardised growth curve (SGC) for De determination on quartz from the Chinese Loess Plateau. *Radiation Measurements*, 41(1): 9-16.

[19] Roberts H and Duller G A. Standardised growth curves for optical dating of sediment using multiple-grain aliquots[J]. *Radiation measurements*, 2004, 38(2): 241-252.

[20] Liu W, Lai Z, Hu K, et al. Age and extent of a giant glacial-dammed lake at Yarlung Tsangpo gorge in the Tibetan Plateau[J]. *Geomorphology*, 2015, 246(1): 370-376.

[21] Prescott J R and Hutton J T. Cosmic ray contributions to dose rates for luminescence and ESR dating: large depths and long-term time variations[J]. *Radiation measurements*, 1994, 23(2-3): 497-500.

[22] Lai, Z. and Brückner, H. Effects of Feldspar Contamination on Equivalent dose and the Shape of Growth Curve for OSL of Silt-Sized Quartz Extracted from Chinese Loess. *Geochronometria*, 2008, 30: 49-53.

[23] Costa J E and Schuster R L. The formation and failure of natural dams[J]. *Geological Society of America Bulletin*, 1988, 100(7): 1054-1068.